JOC The Journal of Organic Chemistry

Article

pubs.acs.org/joc

Synthesis of a Suite of Bioorthogonal Glutathione S-Transferase Substrates and Their Enzymatic Incorporation for Protein Immobilization

Alden E. Voelker and Rajesh Viswanathan*

Department of Chemistry, Case Western Reserve University, Millis Science Center: Rm 216, 2074 Adelbert Road, Cleveland, Ohio 44106-7078, United States

Supporting Information

ABSTRACT: Label-free protein immobilization allows precise detection of biomolecular events. Preserving enzyme function is intrinsically challenging for these strategies. Considering that glutathione S-transferase (GST) is a broadly employed enzymatic fusion tag, we reported a label-free self-catalyzed immobilization for *Schistosoma japonicum* GST. We now report the synthesis, structure, and enzymology of a set of 20 smSNAREs (*s*mall *m*olecule S_NAr-*e*lectrophiles). These smSNAREs mimic (electronically) the canonical GST substrate 1-chloro-2,4-dinitrobenzene (CDNB), and bear a wide variety of bioorthogonal functionalities such as alkynes, aldehydes, acetals, and azides. Sixteen analogues including the chloro- and nitro-substituted **1**, **3**, **5**, **6**, **7**, **11**, **12**, and **13** participated in the GST-catalyzed conjugation, indicating the substrate tolerance of the enzymatic H-site of *Sj*GST. Using UV−vis spectroscopy, we estimate the efficiency of conjugation as a function of substrate diversity. Using LC−MS, we characterized the conjugates formed under each enzymatic transformation. Significant deviations from the canonical CDNB architecture are tolerated. Relative rates between nitro and chloro substituents indicate the nucleophilic addition step is rate determining. Enzyme immobilization on glass slides is affected by additional surface interactions and therefore does not reflect kinetic profiles observed in solution. This new class of heterobifunctional linkers enables a single-step and uniform protein capture on designer surfaces.

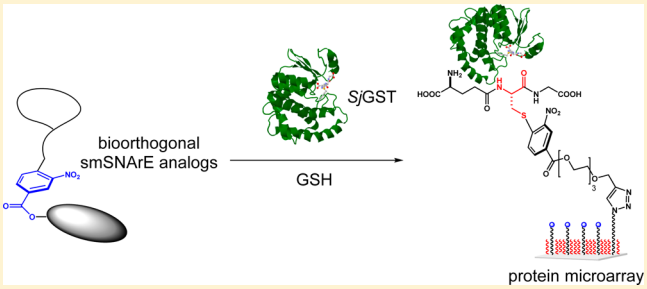

INTRODUCTION

Protein Immobilization through Enzymatic Conjugation. Microarrays and biocatalytic enzyme chips are valuable tools for studying biomolecular events in a high-throughput, resource-economic fashion.[1−8] As the amount of proteomic data available from genome-sequencing studies continues to grow, there is increasing need for robust and selective biochip fabrication technologies.[9] Label-free protein immobilization strategies are particularly valuable for reliable detection of biomolecular events and catalysis occurring in analytes on surfaces.[10] Microfluidic catalysis also benefits from the uniform and selective layering of biocatalysts on surfaces. As compared to DNA microarrays, which have been revolutionary in their own right,[11] the construction of protein biochips is uniquely challenging due to difficulties in selectively and uniformly orienting proteins on surfaces. The need to maintain enzyme function is an intrinsic challenge in biochip fabrication. While it is perhaps impractical to expect one strategy to fit every need in protein biochip technology, several unique methods have been developed to address the challenges posed by the diversity of amino acid functional groups of protein side chains.[12−19] Understandably, the field of engineering innovative enzymatic strategies for selective protein immobilization continues to grow.

***Sj*GST-Catalyzed Selective and Uniform Biochip Formation.** The GST-fusion construct, at the time of its inception, revolutionized protein biochemistry.[20] Among the traditional uses of recombinant protein-fusions, including GST tags, are solubility enhancement, purification, and detection. These tags are now employed nontraditionally for fluorescence labeling in vivo, bioconjugation, and imaging applications.[21] For instance, GST fusion tags have been elegantly used for selective protein immobilization in work by Maynard et al.[22,23] GSTs also have been subjected to bioconjugation and immobilization to produce biocatalytic chips on glass surfaces.[24] We recently reported the development of a self-catalytic protein immobilization strategy using *Schistosoma japonicum* glutathione S-transferase (*Sj*GST) fusion proteins and engineered smSNARE probes.[25] Our mechanism-based approach is schematically outlined in Figure 1.

This protein immobilization technology exploits the enzyme-catalyzed conjugation of glutathione (GSH) to small molecule S_NAr electrophile (smSNARE) substrates. The potential increase in binding affinity between *Sj*GST and the product of the catalytic step after conjugation of smSNAREs to GSH enables the binding of GST or its fusion proteins to surfaces,

Received: June 13, 2013
Published: August 28, 2013

dx.doi.org/10.1021/jo401278x | *J. Org. Chem.* 2013, 78, 9647−9658

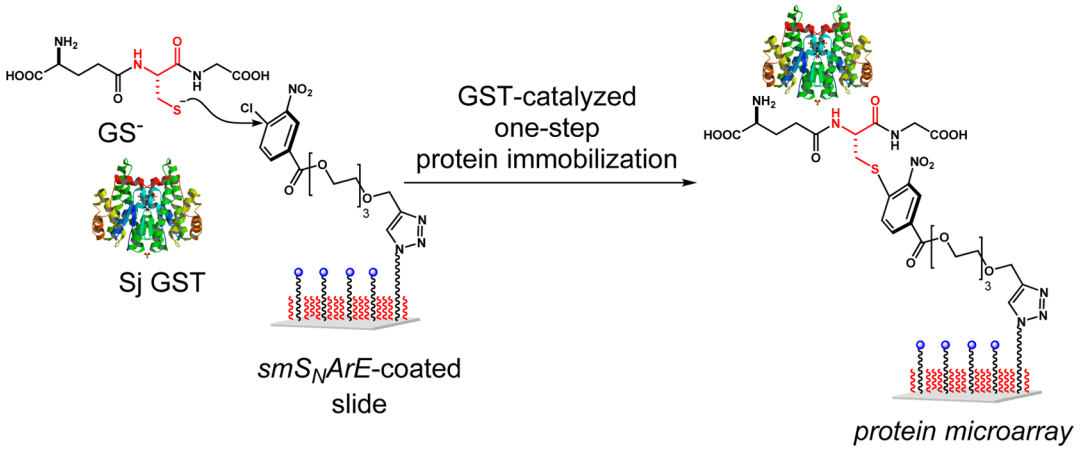

Figure 1. GST-catalyzed protein immobilization using electrophilic surface probes.

leading to a one-step capture event. With the aim of broadly applying this technique to the future bioconjugation of unique materials such as imaging agents and other probes, we created a suite of GST substrate analogues and tested them for enzymatic incorporation. Herein, we describe the synthesis, characterization, and enzymatic incorporation of a set of 20 smSNARE analogues of the canonical GST substrate 1-chloro-2,4-dinitrobenzene (CDNB). These smSNAREs bear a variety of bioorthogonal functionalities[26] such as alkynes, aldehydes, acetals, and azides. A majority of these analogues participate in enzymatic *Sj*GST-catalyzed conjugation reactions with GSH. We report the use of such probes in surface modifications of glass slides and show that protein immobilization can be performed under mild conditions. Further, we compare the conjugation profiles of various substrates in solution and immobilized on glass to conclude that correlations are difficult to draw between these different reaction environments. Overall, these analogues and their conjugation products illustrate the tolerance of the enzymatic active site toward structural modifications of substrates.

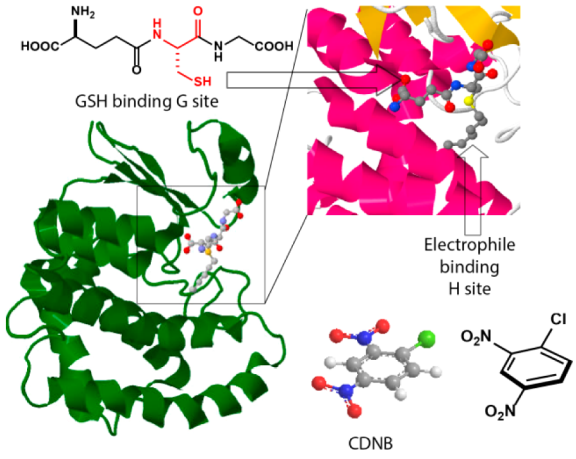

Figure 2. Structure of *Sj*GST. PDB code: 1GTA. X-ray structure (green) at 2.18 Å resolution. Protein crystallized with S-hexyl glutathione. G-site binding to glutathione and H-site binding to electrophile are shown in the active site (magenta).

RESULTS AND DISCUSSION

Design and Engineering *Sj*GST Substrate Analogues. *Sj*GST is a member of the superfamily of multifunctional isoenzymes, known as glutathione S-transferases (GSTs), catalyzing the conjugation of GSH to xenobiotic electrophile. The enzyme-catalyzed reaction proceeds though an S_NAr (*s*ubstitution *n*ucleophilic *ar*omatic) reaction.[27−29] GSH conjugation to electrophiles serves as the first step in the mercapturic acid biosynthesis pathway, eventually leading to detoxification and export across the cell membrane. The canonical substrate CDNB is usually employed as a standard to tease out the catalytic efficiency and the substrate diversity of GSTs.[30] Based on analyses of the X-ray crystal structure of *Sj*GST bound to S-hexyl-GSH[31] as well as observation of trends in the biophysical folding of the protein,[32] we projected the electrophile binding site (H-site) of the enzyme would accommodate a broad range of substrates as shown in Figure 2. We envisioned using appropriate electrophilic probes to serve as "snares" to capture proteins fused to *Sj*GST.[25]

The underlying design elements for the library of electrophiles were the following: first, the molecules preferably must retain a high level of electrophilicity for the GSH conjugation to occur efficiently and second, the analogues should contain bioorthogonal functionalities to act as effective linkers for immobilizing proteins. Therefore, a library of smSNARE substrate candidates was designed as functionalized esters of either 4-chloro-3-nitrobenzoic acid (CNBA) or 3,4-dinitrobenzoic acid (DNBA). Thiol-, alcohol-, and alkyne-functionalized derivatives were synthesized directly from the nitrobenzoic acids, while most other functionalities were derived from ethylene glycol esters.

Synthesis of Bioorthogonal Substrate Analogues. CNBA and DNBA were convenient starting compounds for the synthesis of a diverse library of bioorthogonal functionalities. The syntheses of electrophilic *Sj*GST substrate analogues containing ethylene glycol esters, aldehydes, and acetals are presented in Scheme 1. Activation of CNBA with thionyl chloride produced the corresponding acid chloride (not shown) in situ, which was subsequently treated with ethylene glycol and a catalytic amount of DMAP (10 mol %) to afford monoethylene glycol ester **1-Cl** in 37% yield. The acid functionality of DNBA was similarly transformed to the corresponding acid chloride, which was then treated with ethylene glycol (and DMAP, 10 mol %), resulting in the formation of nitro monoethylene glycol ester **1-NO_2** in 46% yield. Installation of a bioorthogonal aldehyde functionality on monoglycol esters **1-Cl** and **1-NO_2** was performed through a Dess−Martin periodinane oxidation[33] in dichloromethane at

dx.doi.org/10.1021/jo401278x | J. Org. Chem. 2013, 78, 9647−9658

Scheme 1. Synthesis of Aldehyde and Acetal smSNARE Probes 1, 2, and 3

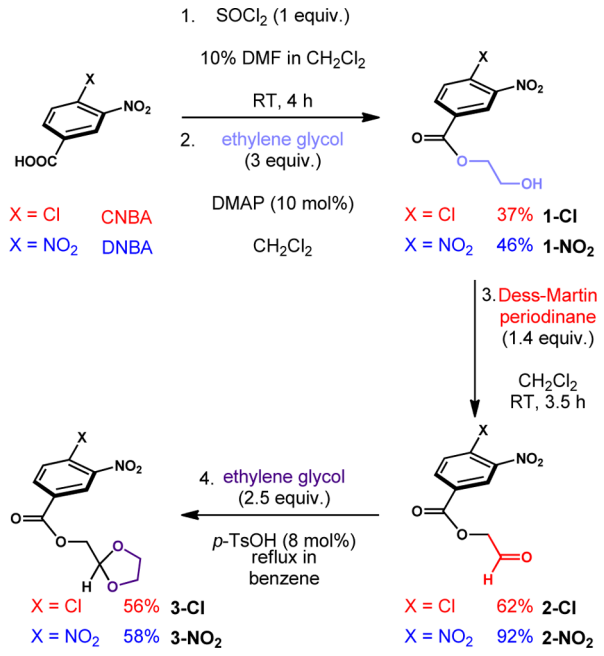

Scheme 2. Synthesis of Iodo and Azide smSNARE Probes 5 and 6

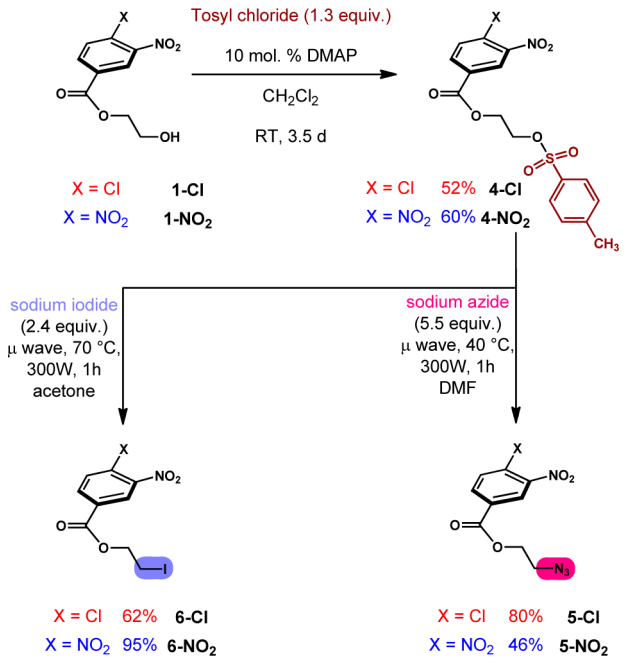

room temperature to result in aldehydes **2-Cl** and **2-NO$_2$** in 62% and 92% yield, respectively.

Masking of the reactive aldehyde functionality of **2-Cl** and **2-NO$_2$** as the corresponding acetals **3-Cl** and **3-NO$_2$** was executed through treatment with slightly superstoichiometric quantities of monoethylene glycol in the presence of a catalytic amount of *p*-toluene sufonic acid in refluxing benzene. Acetals **3-Cl** and **3-NO$_2$** were obtained in 56% and 58% yield, respectively.

Bioorthogonal azide and iodide functional groups were installed through the synthetic transformations illustrated in Scheme 2. Monoethylene glycol ester **1-Cl**, bearing an aromatic chloride substituent, was tosylated using tosyl chloride and catalytic DMAP at room temperature. The corresponding tosylate **4-Cl** was obtained after flash column chromatography as a stable derivative in 52% yield. The appearance of the proton signals corresponding to the aromatic subunit of the tosylate group (^{1}H NMR analysis) provided sufficient proof of the installation of this functionality. Tosylate **4-Cl** was subjected to a nucleophilic substitution reaction with excess sodium azide (5.5 equiv) under microwave irradiation conditions at 40 °C at 300 W for 1 h in DMF, providing the corresponding azido CNBA derivative **5-Cl** in 52% yield. Conversion of tosylate **4-Cl** to the iodide derivative **6-Cl** in 52% yield was achieved through a substitution reaction with excess sodium iodide (2.4 equiv) under microwave irradiation conditions at 70 °C at 300 W over 1 h in acetone.

Similarly to the CNBA-derived chloro analogues, the monoethylene glycol ester of DNBA, **1-NO$_2$**, was converted to the corresponding tosylate **4-NO$_2$** in 60% yield (after flash chromatography) upon treatment with tosyl chloride and DMAP. Azide formation was carried out by treatment of tosylate **4-NO$_2$** with sodium azide under the same microwave conditions used for the formation of azide **5-Cl**, giving azide **5-NO$_2$** in 46% yield after purification by flash chromatography. Iodide formation was carried out in a similar fashion (analogously to iodide **6-Cl**) by treatment of tosylate **4-NO$_2$** with sodium iodide under microwave-mediated reaction conditions. Dinitro analogue **6-NO$_2$** was thus obtained in 95% yield. For compounds **5-Cl** and **5-NO$_2$**, the presence of the azide functionality was indicated through the presence of azide-specific asymmetric stretching bands (2117 and 2111 cm^{-1}) in the IR spectrum.

As illustrated in Scheme 3, triethylene glycol esters of CNBA and DNBA were synthesized in a direct manner similar to the synthesis of their monoethylene glycol ester counterparts (**1-Cl** and **1-NO$_2$**). Treatment of CNBA and DNBA with thionyl chloride to activate the acid functionality followed by addition of triethylene glycol in the presence of catalytic amounts of DMAP (10 mol %) resulted in the formation of esters **7-Cl** and **7-NO$_2$** in 24% and 53% yield, respectively. Thiol-bearing glycol derivatives of CNBA and DNBA were also targeted for synthesis. Treatment of CNBA with thionyl chloride (to activate the acid functionality) in the presence of *β*-mercaptoethanol at −20 °C resulted in the formation of the thiol analogue **8-Cl** in 25% isolated yield. The corresponding

Scheme 3. Synthesis of Triethylene-Glycol Ester and Thiol smSNARE Probes 7 and 8

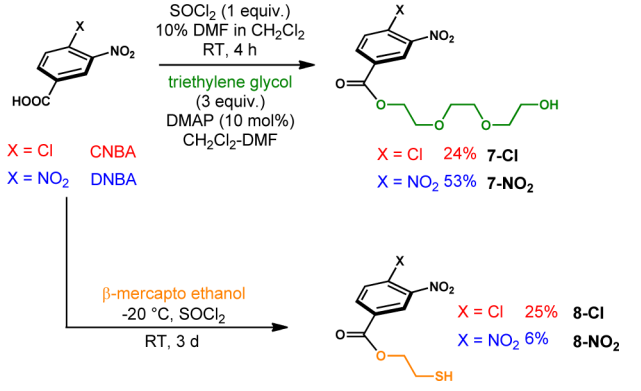

dx.doi.org/10.1021/jo401278x | J. Org. Chem. 2013, 78, 9647−9658

dinitro thiol analogue **8-NO$_2$** was synthesized under similar conditions, resulting in the formation of the product in 6% overall yield. A significant quantity of intractable thiol-oxidation products diverted this pathway to result in a low yield of the desired product.

Three types of bioorthogonal alkyne-containing tethers were designed as esters of CNBA and DNBA. Scheme 4 illustrates

Scheme 4. Synthesis of Alkyne-Containing smSNARE Probes 11, 12, and 13

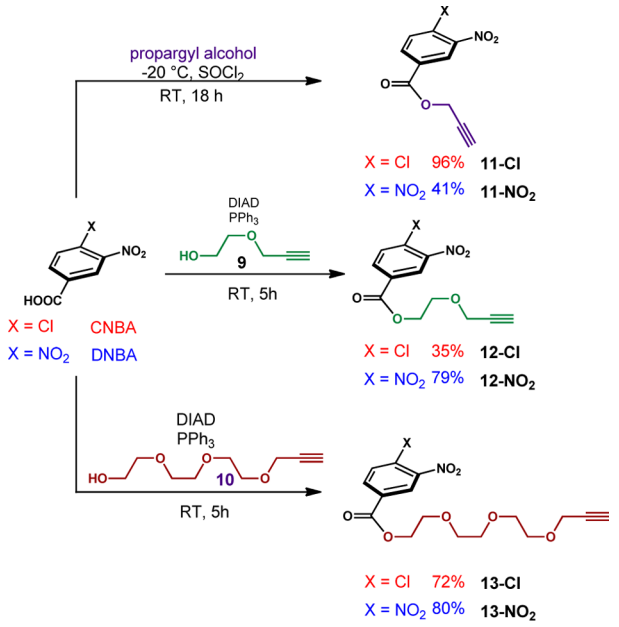

the synthetic routes by which these analogs were accessed. Similar to the conditions for formation of ethylene glycol esters, CNBA yielded propargyl ester **11-Cl** in 96% yield upon treatment with thionyl chloride in excess propargyl alcohol. The nitro-counterpart DNBA provided the dinitro propargyl ester analogue **11-NO$_2$** in 41% yield under similar conditions. In both cases, the presence of the alkyne functionality was evident from the ^{1}H NMR signal in the sp^3 C−H region. A longer tether was also designed to aid in protein immobilization. A Mitsunobu procedure involving initial activation of alcohol **9** using DIAD and triphenylphosphine was planned for the synthesis of CNBA derivative **12-Cl**. Prior to execution of the Mitsunobu reaction, requisite propargyl monoethylene glycol ether **9** was prepared using a straightforward alkylation procedure from ethylene glycol and propargyl bromide.[34] The Mitsunobu reaction proceeded in THF after addition of DIAD to the solution containing propargyl ethylene glycol ether **9**, and resulted in the formation of ester **11-Cl** in 35% yield after isolation through silica gel chromatography. DNBA participated in a similar reaction to give ester **11-NO$_2$** in 79% yield. Rather than employing esterification methods requiring a large excess of alcohols **9** and **10**, the Mitsunobu reaction served as a resource-economic alternative for compounds in the **11** and **12** series, respectively. Similarly, the propargylated triethylene glycol ether **10** was prepared under Williamson ether synthesis from triethylene glycol and propargyl bromide. Upon treating CNBA with **10** under Mitsunobu conditions, the propargylated triethylene glycol ester of CNBA **13-Cl** was obtained in 72% isolated yield. In the same way, treatment of DNBA with alcohol **10** under Mitsunobu conditions gave ester **13-NO$_2$** in 80% yield.

Enzymatic Incorporation of Substrate Analogues. Following the library synthesis, the compounds were assayed for activity with *Sj*GST. A majority of the bioorthogonal substrate analogues participated in the enzymatic transfer reaction and underwent conjugation with GSH. Table 1 shows the results of enzymatic reactions involving the chloro- and nitro series of GST substrate analogues **1**, **3**, **5**, **6**, **7**, **11**, **12**, and **13**. Jakoby's studies have shown that the conjugation of GSH to canonical CDNB substrate is accompanied by a new λ_{max} the UV−vis absorption spectrum at 340 nm.[30] On the basis of this observation, the assay conditions for testing these new analogs were adapted from recent studies reported by Li and co-workers.[35] The enzymatic assay was initiated by addition of 0.5 mM electrophile (150 μL of a 10 mM stock) to a preformed solution of GSH (reduced form, 5 mM) and 300 nM *Sj*GST in 20 mM phosphate buffer, pH 7.0 at 25 °C (eq 1, Table 1). The corresponding nonenzymatic assay mixture contained all components except *Sj*GST. Although the enzyme-catalyzed conjugation progressed significantly after the first few hours, each reaction was allowed to incubate over an 18 h period to ensure maximum conversion to the product. The change in UV absorbance in the 360 nm region was observed for the reaction mixture, allowing the colorimetric detection of product formation. Sixteen of the 20 analogues studied displayed this new absorption peak near 360 nm in the UV−vis absorption spectrum (Table 1, entries 1−16). For each substrate participating in the enzymatic reaction, Table 1 lists the corresponding UV−vis trace (*Y*-axis, absorbance; *X*-axis, wavelength in nm). The ratios of absorbances between the corresponding peaks between each pair of nitro and chloro analogues are presented as an indication of relative rate, in addition to the corresponding MS peak observed for the conjugate. For each analogue, the UV−visible spectrum was compared to the nonenzymatic reaction, which was negligible in most cases. The relative rate of conjugate formation was measured directly by calculating the ratios of absorbance values at the new λ_{max} for each conjugate. For each reaction, residual absorbance in the near 360 nm range, due to the presence of the unreacted electrophile, was subtracted from the absorbance values measured for the reaction mixture. Because of the fact that the assay conditions were identical between the chloro and nitro series, and that the nonenzymatic rates were negligible, the UV absorbance values in each transformation reflected the quantity of conjugate formed. In each case where UV−vis data indicated conjugation, LC−MS analysis of the mixture served as confirmation for the products formed from the enzymatic reactions (see the Supporting Information). Besides the desired products of conjugation (generically represented as **GS-*X*** where ***X*** = 1, 3, 5, 6, 7, 11, 12, and 13; Table 1 bottom), LC−MS traces of reaction mixtures showed the GSH disulfide dimer (GSSG, M$^+$ = 612.15) as the only observable byproduct of this enzymatic assay (data not shown).

Analogues **1**, **3**, **5**, **6**, **7**, **11**, **12**, and **13** participated in the conjugation reaction. Although alcohols **1-Cl** and **1-NO$_2$** participated in the enzyme-catalyzed conjugation reaction with GSH, aldehydes **2-Cl** and **2-NO$_2$** did not. Upon protecting the aldehydes as their ethylene glycol acetals **3-Cl** and **3-NO$_2$**, conjugation proceeded as observed through UV analysis. This result prompts us to propose that the cross-reactivity of the aldehyde functionality with nucleophilic side chains of *Sj*GST is a probable cause for not observing any reaction at the

dx.doi.org/10.1021/jo401278x | J. Org. Chem. 2013, 78, 9647−9658

Table 1. Enzymatic Incorporation Assay Results for smSNARE Probes[a]

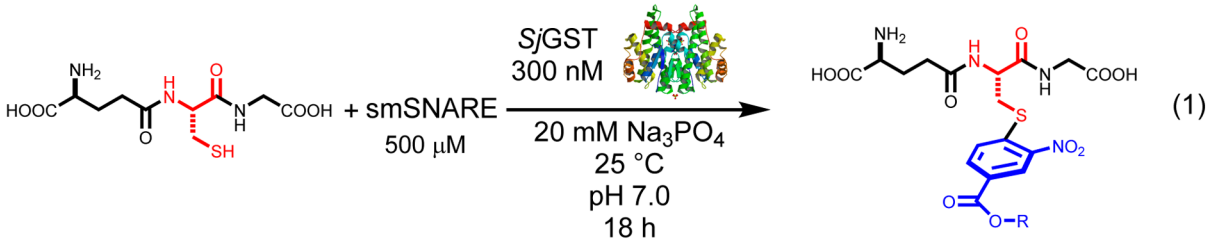

Entry	SjGST substrate analog	GSH-conjugate / product	relative rate (NO_2 : Cl)	Pdt	LC-MS expected	LC-MS found
1 2	**1-Cl** **1-NO_2**	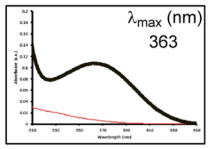	2.5 : 1	**GS-1**	516	515
3 4	**3-Cl** **3-NO_2**	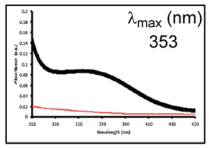	0.8 : 1	**GS-3**	558	557
5 6	**5-Cl** **5-NO_2**	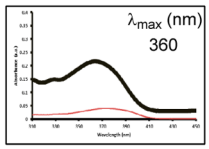	1.2 : 1	**GS-5**	541	539
7 8	**6-Cl** **6-NO_2**	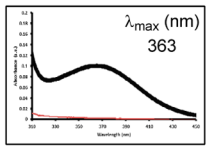	3.0 : 1	**GS-6**	626	625
9 10	**7-Cl** **7-NO_2**	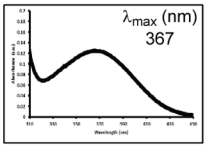	4.6 : 1	**GS-7**	604	605
11 12	**11-Cl** **11-NO_2**	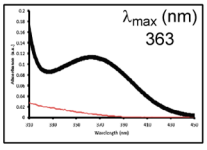	3.4 : 1	**GS-11**	510	509
13 14	**12-Cl** **12-NO_2**	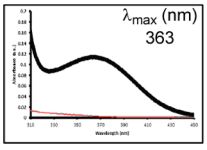	2.5 : 1	**GS-12**	554	553
15 16	**13-Cl** **13-NO_2**	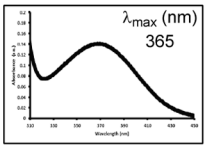	2.6 : 1	**GS-13**	642	643

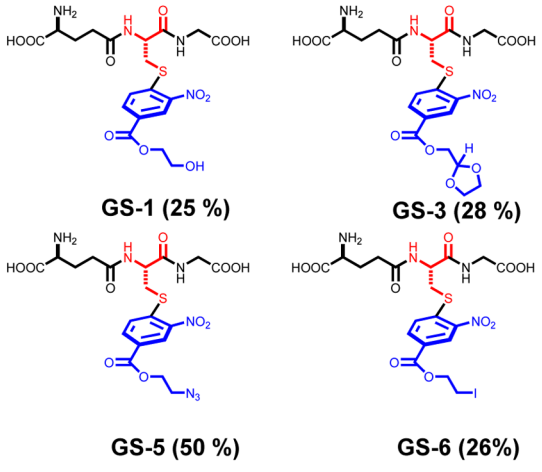

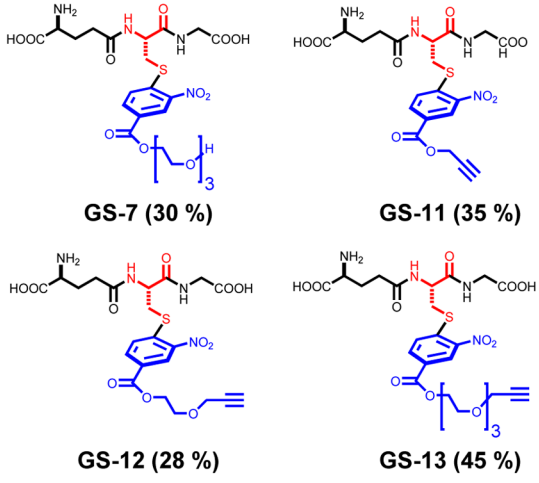

[a]Equation 1 denotes the common enzymatic step. Table lists UV spectra of reactant (red) and product (black), relative ratios, and LC−MS peaks of products. All UV spectra shown above have *X*-axis as wavelength in nm and *Y*-axis as absorbance intensity. Bottom list shows product structures. Yield of conjugate given in parentheses. Yield calculated from UV absorbance data.

electrophilic position of the aromatic ring for the aldehyde-containing substrate analogues **2-Cl** and **2-NO_2** (see Figure S1 in the Supporting Information). Considering the stability and reactive nature of the tosylate functionality, **4-Cl** and **4-NO_2** were not tested for enzymatic incorporation. Instead, they served as precursors for the formation of the iodo and azido analogues (**5** and **6**, respectively). The thiol containing electrophiles **8-Cl** and **8-NO_2** displayed relatively weak participation under the enzymatic assay.

The chloro and the nitro series of analogues displayed a consistent trend in their relative rates of conjugation to GSH. In all cases except **3-Cl**:**3-NO_2** and **5-Cl**:**5-NO_2**, where the relative rates are nearly equal, we observed the nitro series of analogues display modestly enhanced reactivity, from 2.5 to 4.6-

dx.doi.org/10.1021/jo401278x | J. Org. Chem. 2013, 78, 9647−9658

fold. We attribute this increase to two factors: (1) increased electrophilicity shown by nitro-substituted derivatives for the 4-position of the aryl ring (see Figure 3) and (2) increased solubility in assay buffer displayed by the nitro series of substrates.

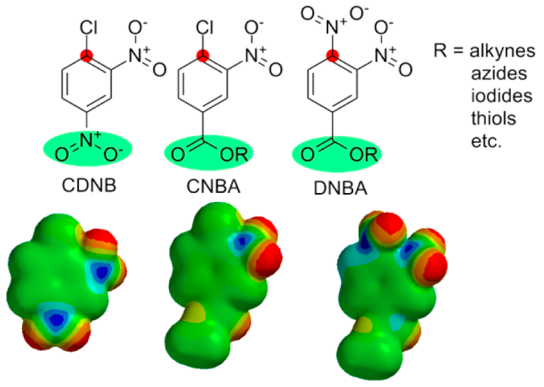

Figure 3. Comparison of electrophilic nature of CNBA and DNBA to CDNB.

Although most of the compounds underwent conjugation to GSH to some degree, qualitative observations indicated that the solubility of the analogues in the phosphate buffer solution played a significant role in the extent and rate of the reaction. Compounds that precipitated even slightly from the solution, such as the thiols (**8-Cl** and **8-NO$_2$**), acids CNBA and DNBA, and CNBA derivatives with short chain ethylene glycol tether (**1-Cl** and **7-Cl**), were less likely to be conjugated to GSH. The entire series of DNBA derivatives were more water-soluble and reacted faster than their corresponding CNBA esters reflected in the ratios depicted in Table 1.

Kinetic Behavior of Select smSNARE Probes. To evaluate the suitability of the synthesized smSNARE compounds as candidates for protein immobilization, as well as the tolerance of *Sj*GST toward increasing linker length, the Michaelis–Menten kinetics for the conjugation of glutathione to three most-soluble smSNAREs were studied. Extinction coefficients for the GSH conjugates were obtained from standard curves made by plotting the absorbance of solutions of the smSNARE electrophiles at different concentrations that had been incubated with glutathione and *Sj*GST at 37 °C overnight. Because of significant insolubility of the electrophiles at concentrations higher than approximately 4 mM, direct linear regression of initial rate data was not possible; rather, Lineweaver–Burk analysis was used to obtain the Michaelis–Menten parameters as shown in Table 2. We found that the reaction rate is generally higher for more-soluble electrophiles, consistent with the notion that the reaction rate depends on the substrate being able to access the active site in solution. Interestingly, alkyne **13-Cl** was found to have a lower K_m than

Table 2. Kinetic Parameters for Select smSNARE Probes[a]

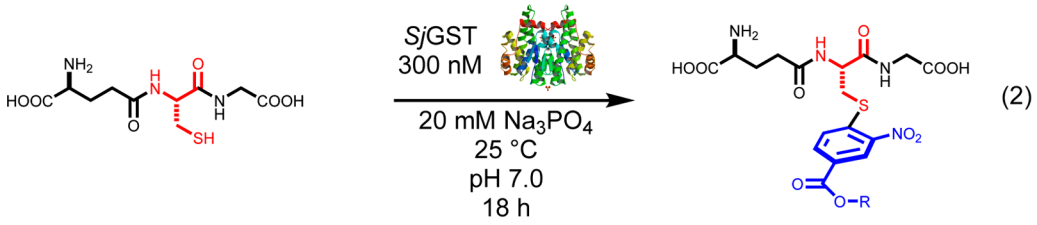

Entry	Electrophile	Extinction coefficient (ε_{356}, $M^{-1}\cdot cm^{-1}$)	K_m (mM)	Vmax (mmol·min-1)	k_{cat} (sec^{-1})	k_{cat}/K_M $mM^{-1}\cdot sec^{-1}$	k_{rel}
1	**1-Cl**	1,791	17.1	0.021	389	23	1.0
2	**1-NO$_2$**	2,081	0.67	0.169	3129	4670	203
3	**13-Cl**	983	6.52	0.031	574	88	3.83

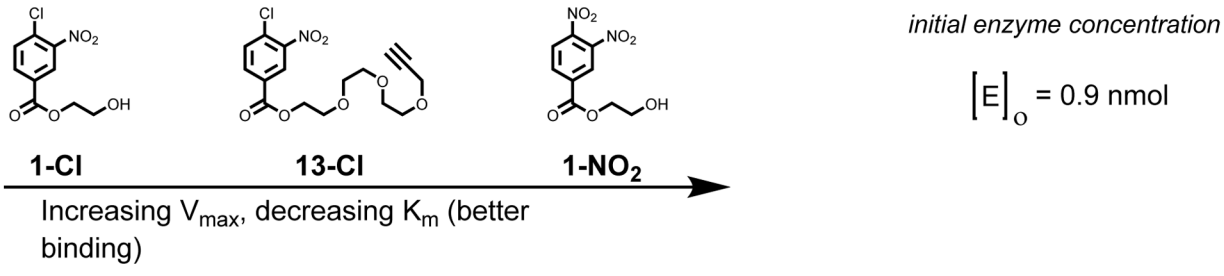

[a]Extinction coefficient calculated from UV analysis at 356 nm. All kinetic parameters are calculated from Lineweaver–Burk plots.

dx.doi.org/10.1021/jo401278x | J. Org. Chem. 2013, 78, 9647–9658

alcohol **1-Cl**, despite the length of its hydrophobic propargyl linker "tail". This may in fact reflect an interaction between the alkyne and the hydrophobic H-site of the *Sj*GST active site. Consistent with enzymatic incorporation studies (Table 1), the kinetic parameters confirmed that the nitro-derivative **1-NO$_2$** is a much better substrate than their chloro counterpart (relative rate of >200-fold between entries 2 and 1 in Table 2). The solubility constants K_{sp} for each of the electrophile may be used in future studies as a relatively more reliable parameter to guide the selection of effective surface probes.

Surface Modifications and Protein Immobilization. Construction of a GST-biochip is shown in Scheme 5. Glass

Scheme 5. GST Protein Immobilization with smSNARE Probes[a]

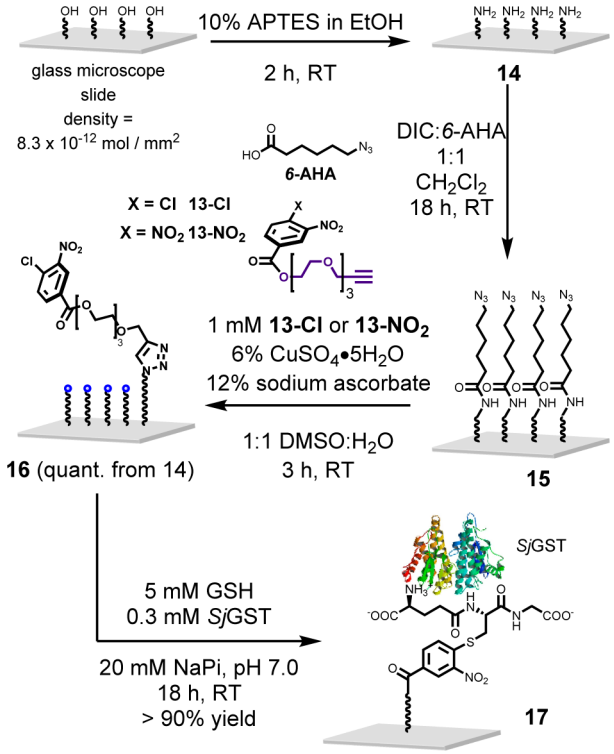

[a]Surface density of immobilized GST = 250 pmol/mm^2.

microscope slides were first treated with (3-aminopropyl)-triethoxysilane (APTES), leading to amine-coated slides (**14**). This step was followed by the carbodiimide-mediated coupling of 6-azidohexanoic acid to produce an azide-bearing surface (**15**). An alkyne-bearing smSNARE was clicked to azide-coated slide **15**. The presence of azides on the surface was confirmed according to our recently documented fluorescence-based analysis.[25] The click reaction on azide-coated surface proceeded in the presence of 1 mM alkyne counterpart **13-Cl** or **13-NO$_2$**, 6% $CuSO_4$ pentahydrate as the requisite metal catalyst, and 12% sodium ascorbate as the reducing agent, producing a glass chip consisting of immobilized electrophilic substrates of *Sj*GST. All of the steps involved in glass surface modification are easy to perform and result in surfaces represented by **16** within 24 h from microscope slides. Quantitative yield was observed in functionalizing the slides starting from **14**. We recently reported construction of GST biochips using surface probes like **16**. Treatment of surface **16** with *Sj*GST and GSH followed by fluorescence immunolabeling showed that the GST is immobilized successfully and with higher efficiency in comparison to epoxy surfaces.[25]

The GST-smSNARE strategy has proven to be advantageous for creating arrays of immobilized proteins, showing an 18-fold increase in fluorescence upon immunolabeling versus non-oriented proteins. In contrast to existing GST-based protein immobilization techniques, this GST-smSNARE strategy combines the conjugation and binding events in one step. The linker functionalities are highly tunable for a variety of common conjugation strategies, yet the CDNB-like moiety allows proteins to be bound in a specific manner. To evaluate the robustness of the enzyme binding on the surface, slides bearing immobilized *Sj*GST were treated with 100 mM GSH in phosphate buffer (20 mM, pH 7.0) or 1% sodium dodecyl sulfate in glycine buffer (200 mM, pH 2.0) for 1 h, then immunolabeled and imaged. In both cases, fluorescent signals were observed, indicating that the enzyme remained bound to the surface.

While it is reasonable to consider the possibility that protein containing surface cysteines with low pK_a might be competing for smSNARE electrophiles, we do observe high selectivity for GST immobilization due to the fact that GSH is required for this immobilization, and the binding between GSH and GST is well-known to be specific, thereby rendering inherent selectivity to this strategy. An upper limit for the immobilized *Sj*GST concentration is estimated on the basis of the surface density of smSNARE analogues present on the glass surface. Considering that we saturate the linker solutions during functionalization of the slide (**14** to **15** to **16**), on the basis of surface density of alcohols present on slides at the beginning, we estimate the surface density of smSNAREs to be 8.3×10^{-12} mol/mm^2 in **16**. On the basis of the fluorescence intensity readout, we measure for respective antibody concentrations (data not shown), and on the bassi of the fact that 59 mm^2 is the area for each spot on the array, the density of immobilized *Sj*GST is 442 pmol. This corresponds to a 90% yield of immobilized *Sj*GST. In this study, we prepared surfaces represented by **16** containing different smSNAREs for comparison of their respective kinetic parameters and their influence on surface immobilization. Figure 4 shows the results of this comparative analysis. Surfaces prepared with smSNARE **13-Cl** were compared to **13-NO$_2$**, and *Sj*GST immobilization and immunolabeling were performed as previously reported.[25] On the basis of superior kinetic profiles of most nitro-substituted electrophiles in solution, we anticipated **13-NO$_2$** to display higher density and therefore intensity of fluorescence signal. To our surprise, **13-Cl** displayed a slightly enhanced intensity (by a factor of ~1.5-fold). We attribute this result to the fact that conjugation of *Sj*GSTs on a solid support inherently involves multiple factors that are not encountered in solution-based kinetics studies. In essence, comparative analyses like this study underscore the often overlooked importance of enzyme–surface interactions other than the protein–linker interaction that are encountered during immobilization.

Aromatic halides and glutathione derivatives have previously been studied as potential substrates or inhibitors for a variety of GST isoforms.[36−39] While substrate tolerance differs among individual enzymes, the best aryl halide substrates for *Sj*GST in an extensive study by Lo et al. were those bearing a substituent that is electron withdrawing via resonance, like a nitro moiety.[35] The electrophilic esters described in our study share this structural feature. Fujikawa et al. used a different GST isoform (the human enzyme hGSTP1) to elegantly study the relative

dx.doi.org/10.1021/jo401278x | J. Org. Chem. 2013, 78, 9647−9658

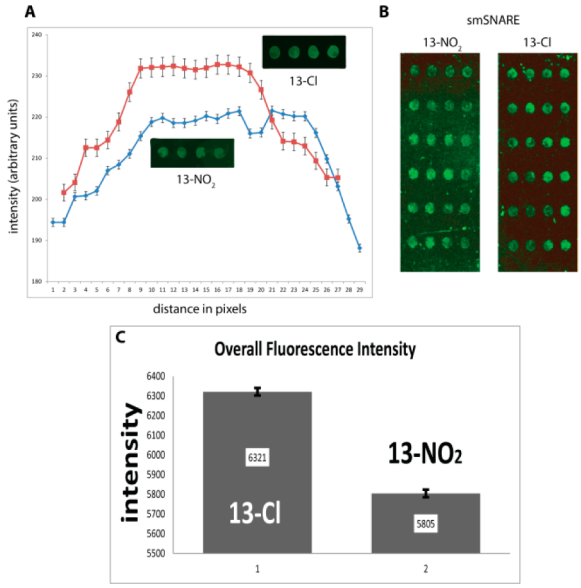

Figure 4. (A) Cross-section of spot intensity from GST protein immobilization with smSNARE probes **13-Cl** and **13-NO$_2$**. (B) Array of spots from *Sj*GST immobilized through **13-NO$_2$** (left) and **13-Cl** (right). (C) Overall intensity of spots from arrays created by immobilizing *Sj*GST on **13-Cl** and **13-NO$_2$**.

rates of conjugation of glutathione to amide and ketone analogues of CNBA and DNBA; it was observed that DNBA derivatives reacted faster than CNBA derivatives.[40] These results correspond to the reactivity profiles measured for the analogues in this study. From a binding and inhibition perspective, studies by Li et al.[35] and Garcia-Fuentes et al.[41] have shown that the best binding to *Sj*GST is achieved by substrates that can interact with both the glutathione-binding G-site and the hydrophobic H-site of the enzyme's active site, and that binding affinity increases by 2 orders of magnitude for S-octylglutathione over S-methylglutathione. Both of these observations in the literature confirm results that we have obtained, and help point the way toward designing a second generation of improved electrophiles for GST tag-based protein immobilizations.

CONCLUSION

We have developed a series of electrophilic substrates for *Sj*GST and studied their potential as linkers for a mechanistically inspired selective protein immobilization strategy. During the course of this work, we have noted that the extent and rate of conjugation appear to correlate with the solubility of the substrate in aqueous media. Our work illustrates proof of hypothesis derived on the basis of analyses of the X-ray crystal structure of *Sj*GST bound to S-hexyl-GSH[31] as well as observation of trends in the biophysical folding of the protein,[32] that the electrophile binding site (H-site) of the enzyme accommodates a broad range of substrates. We take advantage of this tolerance using appropriate electrophilic probes to serve as "snares" to capture proteins fused to *Sj*GST. This work represents the first immobilization strategy that exploits the catalytic and binding properties of the GST tag, commonly used for protein purification purposes. As this tag is easily introduced into virtually any genomic protein via commercially available expression vector systems (pGEX for example), future efforts will be directed toward creating functional arrays of a variety of immobilized enzymes.

EXPERIMENTAL SECTION

General Methods. All reactions were carried out under argon with dry solvents unless otherwise noted. Reactions were monitored by thin-layer chromatography on silica gel plates ($60F_{254}$) with a fluorescent indicator, and visualized with UV light, $KMnO_4$, or 2,4-dinitrophenylhydrazine. Yields refer to chromatographically purified or crystallized compounds. All commercially available reagents were used without further purification. CH_2Cl_2 and THF were dried by activated alumina. Anhydrous benzene 99.8%, Et_2O ACS 99.0%, ethyl acetate ACS 99.5%, hexanes ACS 98.5%, anhydrous DMF 99.8%, and anhydrous NMP 99.5% were purchased and used as received. All synthetic separations were carried out under flash chromatographic conditions on silica gel (230−400 mesh) at medium pressure (20 psi). All new compounds gave satisfactory spectroscopic analyses (IR, ^{1}H NMR, ^{13}C NMR, HRMS). NMR spectra were determined on 300, 400, or 600 MHz spectrometers. ^{1}H NMR spectra are reported in parts per million (δ) relative to the residual solvent peak. Data for ^{1}H are reported as follows: chemical shift (δ ppm), multiplicity (s = singlet, bs = broad singlet, d = doublet, t = triplet, q = quartet, ddd = double double doublet, m = multiplet, cm = complex multiplet), integration, and coupling constant in Hz. ^{13}C NMR spectra were obtained on a 300, 400, or 600 MHz spectrometer and are reported in parts per million (δ) relative to the residual solvent peak. HRMS spectra were obtained on an ESI spectrometer with a quadrupole analyzer. Infrared (IR) (υ, cm^{-1}) spectra were recorded on a Fourier Spectrum FT-IR. Melting points were measured in capillary tubes and are uncorrected. Reverse-phase LC−MS analyses were carried out on a C-18 column (250 × 4.6 mm, 300 Å pore size, 10 μm particle size). For conjugation reactions, *Schistosoma japonicum* glutathione S-transferase (0.1 mg/mL) was purchased and stored as 100 μL aliquots at 4 °C until use. For immunolabeling studies, mouse monoclonal primary anti-GST antibodies and secondary goat monoclonal antimouse antibodies, labeled with Texas Red, were purchased and used as received.

Representative Procedures. *General Procedure A: Synthesis of Ethylene Glycol and Triethylene Glycol Esters.* The appropriate nitrobenzoic acid (ca. 5 mmol) and thionyl chloride (1 equiv) were combined in 20 mL of 10% DMF (*N*,*N*-dimethylformamide) in dry CH_2Cl_2, and stirred under N_2 gas at room temperature for 4 h. To this solution were added either ethylene glycol or triethylene glycol (3 equiv) and DMAP (*N*,*N*-dimethyl-4-aminopyridine, 10 mol %) in 10 mL of dry CH_2Cl_2, and the solution was stirred under N_2 atmosphere at room temperature overnight. Deionized water (10 mL) was added to quench the reaction, and the organic layer was washed with water (2 × 20 mL) and brine (20 mL). The organic layer was dried over $MgSO_4$, and the solvent was evaporated in vacuo. The ester was isolated by elution over a column of silica gel.

General Procedure B: Synthesis of Tosylates. Adapting a procedure from Randl et al.,[42] alcohol **1-Cl** or **1-NO$_2$** (ca. 4−5 mmol), DMAP (10 mol %), tosyl chloride (1.3 equiv), and pyridine (2 equiv) were dissolved in 20 mL of CH_2Cl_2. The solution was stirred at room temperature for 3.5 days, and then concentrated in vacuo. The residue was eluted over silica gel to afford the tosylate.

General Procedure C: Synthesis of Iodides. The appropriate tosylate (ca. 1 mmol) and sodium iodide (2.4 equiv) were combined in acetone (5 mL) and irradiated in a microwave reactor at 70 °C (300 W) for 1 h, whereupon a white precipitate of sodium tosylate was observed at the bottom of the reaction tube. The solution was diluted with 20 mL of ice water and extracted with ether (3 × 20 mL). The combined organic layers were washed with water (20 mL) and brine (20 mL,) then dried over $MgSO_4$ and concentrated in vacuo. The iodide was isolated and purified by elution over a column of silica gel.

General Procedure D: Synthesis of Azides. The appropriate tosylate (ca. 1 mmol) and sodium azide (5.5 equiv) were combined in 5 mL of DMF. The solution was irradiated in a microwave reactor at 40 °C (300 W) for 1 h, and the resulting orange solution was diluted

dx.doi.org/10.1021/jo401278x | J. Org. Chem. 2013, 78, 9647−9658

in ice water (45 mL) and extracted with ether (5 × 20 mL). The combined organic layers were dried with $MgSO_4$, concentrated in vacuo, and eluted over silica gel to afford the azide.

General Procedure E: Synthesis of Aldehydes. A solution of alcohol **1-Cl** or **1-NO$_2$** (ca. 1−2 mmol) in 10 mL of CH_2Cl_2 was added to a solution of Dess−Martin periodinane (1.4 equiv) prepared according to literature protocol[33] in 10 mL of CH_2Cl_2. The reaction was stirred under flowing nitrogen gas at room temperature for 3.5 h, and then the solvent was removed in vacuo. The aldehyde was isolated by elution over silica gel.

General Procedure F: Synthesis of Acetals. Adapting a procedure from Bastian et al.,[43] the appropriate aldehyde (ca. 2−3.5 mmol) and ethylene glycol (2.5 equiv) were combined with *p*-toluenesulfonic acid monohydrate (ca. 8 mol. %) in benzene (25 mL). The reaction was refluxed with a Dean−Stark trap overnight, and the solvent was removed in vacuo. The acetal was isolated by elution over silica gel.

General Procedure G: Synthesis of β-Mercaptoethanol Esters. The appropriate nitrobenzoic acid (ca. 2−5 mmol) was suspended in β-mercaptoethanol (10 mL) under nitrogen gas and chilled to −20 °C. To this suspension was slowly added thionyl chloride (1 equiv), and the reaction was brought to room temperature and stirred for 3 days. The reaction was then diluted with water (20 mL) and extracted into diethyl ether (3 × 20 mL). The combined organic layers were then washed with saturated $NaHCO_3$ (2 × 20 mL) and brine (20 mL), then dried over $MgSO_4$ and concentration in vacuo. The thiol was isolated by elution over silica gel.

General Procedure H: Synthesis of Propargyl Esters. The appropriate nitrobenzoic acid (ca. 1.2 mmol) was dissolved in 5 mL of propargyl alcohol, stirred under N_2 gas, and chilled to −20 °C. To this solution was added thionyl chloride (3 equiv), and the mixture was stirred for 18 h at room temperature. The propargyl ester was isolated by elution over silica gel and recrystallized from boiling ethyl acetate.

General Procedure I: Synthesis of Propargyl Ether Esters.[44] The alkynes were prepared via a Mitsunobu reaction. Diisopropyl azodicarboxylate (DIAD, 1.3 equiv) was added dropwise to a foil-covered flask containing a stirred solution of either propargyl ethylene glycol ether **9** or propargyl triethylene glycol ether **10** (ca. 1−2 mmol), triphenylphosphine (1.3 equiv), and the appropriate nitrobenzoic acid (1.3 equiv) in 10 mL of dry THF. The reaction was stirred under flowing nitrogen gas at room temperature for 5 h. The solvent was removed in vacuo, and the resulting residue was eluted over silica gel to afford the propargyl ether ester.

2-Hydroxyethyl 4-Chloro-3-nitrobenzoate (1-Cl). This was prepared by general procedure A from 4-chloro-3-nitrobenzoic acid (CNBA, 1.0 g, 4.96 mmol) and ethylene glycol (0.83 mL, 3 equiv) in 10 mL of dry CH_2Cl_2. Flash chromatography (50% ethyl acetate/hexanes) and recrystallization from boiling ethyl acetate afforded the ester as an off-white powder in 37% yield (426 mg). MW: 245.62 g/mol. TLC: 50% ethyl acetate/hexanes, R_f = 0.15. ^{1}H NMR (400 MHz, $CDCl_3$): δ 8.51 (d, 1H, J = 2 Hz), 8.17 (dd, 1H, J_1 = 8.4 Hz, J_2 = 2.0 Hz), 7.63 (d, 1H, J = 8.4 Hz), 4.47 (t, 2H, J = 4.8 Hz), 3.95 (t, 2H, J = 4.8 Hz), 1.85 (bs, 1H). ^{13}C NMR (100 MHz, $CDCl_3$): δ 164.2, 148.0, 133.9, 132.4, 132.0, 130.0, 126.8, 67.6, 61.1 ppm. HRMS (ESI, m/z): calcd for $C_9H_9ClNO_5$ $(M + H)^+$ 246.0169; found 246.0174. Mp: 95−96 °C.

2-Hydroxyethyl 3,4-Dinitrobenzoate (1-NO$_2$). This was prepared by general procedure A from 3,4-dinitrobenzoic acid (DNBA, 1 g, 4.71 mmol) and ethylene glycol (0.8 mL, 3 equiv) in 10 mL of dry CH_2Cl_2. Elution over silica gel (ethyl acetate/hexanes, 70%) and recrystallization gave the ester as a yellow powder in 46% yield (555 mg). MW: 256.17 g/mol. TLC: 50% ethyl acetate/hexanes, R_f = 0.30 ^{1}H NMR (400 MHz, $CDCl_3$): δ 8.60 (d, 1H, J = 2 Hz), 8.43 (dd, 1H, J_1 = 8.4 Hz, J_2 = 1.6 Hz), 7.97 (d, 1H, J = 8.4 Hz), 4.55 (m, 2H), 4.00 (m, 2H). ^{13}C NMR (100 MHz, DMSO-d_6): δ 162.8, 144.4, 141.8, 135.2, 134.8, 126.4, 126.2, 68.1, 58.9 ppm. HRMS (ESI, m/z): calcd for $C_9H_9N_2O_7$ $(M + H)^+$ 257.0410; found 257.0396. Mp: 109−110 °C.

2-Oxoethyl 4-Chloro-3-nitrobenzoate (2-Cl). This was prepared by general procedure E from alcohol **1-Cl** (491 mg, 2.0 mmol) in 10 mL of CH_2Cl_2. Elution over silica gel (70% ethyl acetate/hexanes) afforded the aldehyde as yellow oil in 62% yield (302 mg). MW: 243.60 g/mol. TLC: 50% ethyl acetate/hexanes, R_f = 0.19. ^{1}H NMR (400 MHz, $CDCl_3$): δ 9.70 (s, 1H), 8.56 (d, 1H, J = 2.4 Hz), 8.21 (dd, 1H, J_1 = 8.4 Hz, J_2 = 2 Hz), 7.68 (d, 1H, J = 8.4 Hz), 4.98 (s, 2H) ppm.

2-Oxoethyl 3,4-Dinitrobenzoate (2-NO$_2$). This was prepared by general procedure E from alcohol **1-NO$_2$** (512 mg, 2.0 mmol) in 10 mL of CH_2Cl_2. The aldehyde was isolated by elution over silica gel (70% ethyl acetate/hexanes) as yellow oil in 92% yield (468 mg). MW: 254.15 g/mol. TLC: 80% ethyl acetate/hexanes, R_f = 0.43. ^{1}H NMR (400 MHz, $CDCl_3$): δ 9.70 (s, 1H), 8.64 (d, 1H, J = 2 Hz), 8.46 (dd, 1H, J_1 = 8.4 Hz, J_2 = 2 Hz), 7.99 (d, 1H, J = 8.4 Hz), 5.06 (s, 2H) ppm.

(1,3-Dioxolan-2-yl)methyl 4-Chloro-3-nitrobenzoate (3-Cl). This was prepared by general procedure F from aldehyde **2-Cl** (881 mg, 3.62 mmol) and ethylene glycol (0.5 mL, 2.5 equiv). The acetal was isolated by elution over silica gel (50% ethyl acetate/hexanes) as yellow oil in 56% yield (583 mg). MW: 287.65 g/mol. TLC: 50% ethyl acetate/hexanes, R_f = 0.37. ^{1}H NMR (400 MHz, $CDCl_3$): δ 8.50 (d, 1H, J = 2 Hz), 8.17 (dd, 1H, J_1 = 8.4 Hz, J_2 = 2 Hz), 7.63 (d, 1H, J = 8.4 Hz), 5.25 (t, 1H, J = 3.9 Hz), 4.39 (d, 2H, J = 3.9 Hz), 3.98 (cm, 4H). ^{13}C NMR (100 MHz, CDCl3): δ 163.2, 147.8, 133.7, 132.2, 131.7, 129.7, 127.8, 126.6, 100.9, 65.3, 65.1 ppm. HRMS (ESI, m/z): calcd for $C_{11}H_{11}ClNO_6$ $(M + H)^+$ 288.0275; found 288.0257.

(1,3-Dioxolan-2-yl)methyl 3,4-Dinitrobenzoate (3-NO$_2$). This was prepared by general procedure F from aldehyde **2-NO$_2$** (519 mg, 2.0 mmol) and ethylene glycol (0.3 mL, 2.5 equiv). The acetal was isolated by elution over silica gel (50% ethyl acetate/hexanes) as yellow oil in 58% yield (346 mg). MW: 298.21 g/mol. TLC: 70% ethyl acetate/hexanes, R_f = 0.49. ^{1}H NMR (400 MHz, $CDCl_3$): δ 8.55 (d, 1H, J = 1.6 Hz), 8.40 (dd, 1H, J_1 = 8.4 Hz, J_2 = 1.6 Hz), 7.95 (d, 1H, J = 8.4 Hz), 5.23 (t, 1H, J = 4 Hz), 4.41 (d, 2H, J = 4 Hz), 3.96 (cm, 4H). ^{13}C NMR (100 MHz, $CDCl_3$): δ 162.4, 145.4, 142.7, 134.9, 134.8, 126.6, 125.5, 100.9, 65.7, 65.5 ppm. HRMS (ESI, m/z): calcd for $C_{11}H_{11}N_2O_8$ $(M + H)^+$ 299.0515; found 299.0511.

2-(*p*-Toluenesulfoxy)ethyl 4-Chloro-3-nitrobenzoate (4-Cl). This was prepared by general procedure B from alcohol **1-Cl** (1 g, 4.1 mmol). The residue was eluted over silica gel (35% ethyl acetate/hexanes) to afford the tosylate as an off-white powder in 52% yield (846 mg). MW: 399.80 g/mol. TLC: 50% ethyl acetate/hexanes, R_f = 0.38. ^{1}H NMR (400 MHz, $CDCl_3$): δ 8.38 (d, 1H, J = 2 Hz), 8.10 (dd, 1H, J_1 = 8.4 Hz, J_2 = 2 Hz), 7.77 (d, 2H, J = 8.4 Hz), 7.63 (d, 1H, J = 8.4), 7.30 (d, 2H, J = 8 Hz), 4.52 (t, 2H, J = 4.4), 4.35 (t, 2H, J = 4.4), 2.40 (s, 3H). ^{13}C NMR (100 MHz, $CDCl_3$): δ 163.4, 148.0, 145.5, 133.9, 132.7, 132.4, 132.2, 130.1, 129.4, 128.0, 126.8, 67.4, 63.2, 21.8 ppm. HRMS (ESI, m/z): calcd for $C_{16}H_{14}ClNO_7SNa$ $(M + Na)^+$ 422.0077; found 422.0071. Mp: 101−103 °C.

2-(Tosyloxy)ethyl 3,4-Dinitrobenzoate (4-NO$_2$). This was prepared by general procedure B from alcohol **1-NO$_2$** (1.2 g, 4.68 mmol). The tosylate was obtained by elution over silica gel (ethyl acetate/hexanes 50%) as a yellow powder in 60% yield (1.15 g). MW: 410.36 g/mol. TLC: 50% ethyl acetate/hexanes, R_f = 0.26. ^{1}H NMR (400 MHz, $CDCl_3$): δ 8.47 (d, 1H, J = 1.6 Hz), 8.36 (dd, 1H, J_1 = 8.4 Hz, J_2 = 1.6 Hz), 7.95 (d, 1H, J = 8.4 Hz), 7.75 (d, 2H, J = 8.4), 7.31 (d, 2H, J = 8.4), 4.57 (m, 2H), 4.37 (m, 2H), 2.40 (s, 3H). ^{13}C NMR (100 MHz, $CDCl_3$): δ 162.4, 145.6, 145.5, 142.6, 135.0, 134.4, 132.7, 130.2, 128.0, 126.6, 125.6, 67.2, 63.8, 21.8 ppm. HRMS (ESI, m/z): calcd for $C_{16}H_{14}N_2O_9SNa$ $(M + Na)^+$ 433.0318; found 433.0305. Mp: 115−116 °C.

2-Azidoethyl 4-Chloro-3-nitrobenzoate (5-Cl). This was prepared by general procedure D from tosylate **4-Cl** (511 mg, 1.3 mmol) and sodium azide (450 mg, 5.5 equiv). The residue was purified by flash chromatography (50% ethyl acetate/hexanes) to afford the azide as viscous, yellow oil that crystallized in the refrigerator at 4 °C in 80% yield (281 mg). MW: 270.63 g/mol. TLC: 50% ethyl acetate/hexanes, R_f = 0.46. ^{1}H NMR (400 MHz, $CDCl_3$): δ 8.58 (d, 1H, J = 2 Hz), 8.25 (dd, 1H, J_1 = 8.4 Hz, J_2 = 2 Hz), 7.40 (d, 1H, J = 8.4 Hz), 4.52 (t, 2H, J = 5.1 Hz), 3.61 (t, 2H, J = 5.1 Hz). ^{13}C NMR (150 MHz, $CDCl_3$): δ 163.7, 148.1, 139.5, 134.8,

dx.doi.org/10.1021/jo401278x | J. Org. Chem. 2013, 78, 9647−9658

127.9, 126.5, 121.1, 64.6, 49.9 ppm. FTIR (thin film, ν_{max}): 3090, 2965, 2918, 2117, 1721, 1609, 1532, 1347, 1282, 1243, 1119 cm^{-1}. Mp: 54−56 °C.

2-Azidoethyl 3,4-Dinitrobenzoate (5-NO$_2$). This was prepared by general procedure D from tosylate **4-NO$_2$** (409 mg, 1 mmol) and sodium azide (352 mg, 5.4 equiv). The residue was eluted over silica gel (50% ethyl acetate/hexanes) to give the azide as a crystalline orange solid in 46% yield (129 mg). MW: 281.18 g/mol. TLC: 50% ethyl acetate/hexanes, R_f = 0.45. ^{1}H NMR (400 MHz, $CDCl_3$): δ 8.56 (d, 1H, J = 2 Hz), 8.24 (dd, 1H, J_1 = 8.4 Hz, J_2 = 2 Hz), 7.39 (d, 1H, J = 8.4 Hz), 4.51 (t, 2H, J = 5.1 Hz), 3.61 (t, 2H, J = 5.1 Hz). ^{13}C NMR (150 MHz, $CDCl_3$): δ 163.8, 149.1, 139.5, 134.8, 127.9, 126.6, 121.1, 64.6, 50.0 ppm. FTIR (thin film, ν_{max}): 3101, 2956, 2111, 1719, 1610, 1539, 1352, 1297, 1230, 1117, 1114 cm^{-1}. Mp: 54−57 °C.

2-Iodoethyl 4-Chloro-3-nitrobenzoate (6-Cl). This was prepared by general procedure C from tosylate **4-Cl** (354 mg, 0.89 mmol) and sodium iodide (320 mg, 2.4 equiv) in acetone (5 mL). Elution over silica gel (20% ethyl acetate/hexanes) afforded the iodide as a yellow powder in 62% yield (196 mg). MW: 355.51 g/mol. TLC: 50% ethyl acetate/hexanes, R_f = 0.53. ^{1}H NMR (400 MHz, $CDCl_3$): δ 8.51 (d, 1H, J = 2 Hz), 8.17 (dd, 1H, J_1 = 8.4 Hz, J_2 = 2 Hz), 7.65 (d, 1H, J = 8.4 Hz), 4.60 (t, 2H, J = 6.8 Hz), 3.42 (t, 2H, J = 6.8 Hz). ^{13}C NMR (100 MHz, $CDCl_3$): δ 163.2, 148.1, 133.9, 132.5, 132.2, 129.7, 126.9, 65.9, 0.04 ppm. HRMS (ESI, m/z): calcd for $C_9H_8ClINO_4$ $(M + H)^+$ 355.9187; found 355.9182. Mp: 91−93 °C.

2-Iodoethyl 3,4-Dinitrobenzoate (6-NO$_2$). Prepared by general procedure C from tosylate **4-NO$_2$** (409 mg, 1 mmol) and sodium iodide (398 mg, 2.7 equiv) in acetone (5 mL). Elution over silica gel (50% ethyl acetate/hexanes) afforded the iodide as an orange oil that solidified upon standing in 95% yield (348 mg). MW: 366.07 g/mol. TLC: 50% ethyl acetate/hexanes, R_f = 0.54. ^{1}H NMR (400 MHz, $CDCl_3$): δ 8.55 (d, 1H, J = 2 Hz), 8.42 (dd, 1H, J_1 = 8.4 Hz, J_2 = 2 Hz), 7.97 (d, 1H, J = 8.4 Hz), 4.62 (t, 2H, J = 6.6 Hz), 3.43 (t, 2H, J = 6.6 Hz). ^{13}C NMR (150 MHz, $CDCl_3$): δ 162.0, 145.2, 142.4, 134.9, 134.6, 126.4, 125.5, 66.3, −0.17 ppm. HRMS (ESI, m/z): calcd for $C_9H_8IN_2O_6$ $(M + H)^+$ 366.9427; found 366.9428. Mp: 40−43 °C.

2-(2-(2-Hydroxyethoxy)ethoxy)ethyl 4-Chloro-3-nitrobenzoate (7-Cl). This was prepared by general procedure A from CNBA (1 g, 4.96 mmol) and triethylene glycol (2.0 mL, 3 equiv) in 10 mL of DMF/CH_2Cl_2. The ester was isolated by column chromatography (90% ethyl acetate/hexanes) as a light yellow oil in 24% yield (397 mg). MW: 333.72 g/mol. TLC: 80% ethyl acetate/hexanes, R_f = 0.13. ^{1}H NMR (400 MHz, $CDCl_3$): δ 8.53 (d, 1H, J = 2 Hz), 8.18 (dd, J_1 = 8.4 Hz, J_2 = 2 Hz), 7.63 (d, 1H, J = 8.4 Hz), 4.51 (t, 2H, J = 4.8 Hz), 3.83 (t, 2H, J = 4.8 Hz), 3.68 (cm, 8H), 3.59 (t, 2H, J = 4.4 Hz), 2.31 (bs, 1H). ^{13}C NMR (100 MHz, $CDCl_3$): δ 163.3, 147.4, 133.5, 131.9, 131.0, 129.6, 126.2, 72.2, 70.3, 69.9, 68.6, 64.7, 61.2 ppm. HRMS (ESI, m/z): calcd for $C_{13}H_{16}ClNO_7Na$ $(M + Na)^+$ 356.0513; found 356.0523.

2-(2-(2-Hydroxyethoxy)ethoxy)ethyl 3,4-Dinitrobenzoate (7-NO$_2$). This was prepared by general procedure A from DNBA (1 g, 4.71 mmol) and triethylene glycol (1.9 mL, 3 equiv) in 10 mL of DMF/CH_2Cl_2. The ester was isolated by column chromatography (90% ethyl acetate/hexanes) as a yellow oil in 53% yield (859 mg). MW: 344.27 g/mol. TLC: 80% ethyl acetate/hexanes, R_f = 0.19. ^{1}H NMR (400 MHz, $CDCl_3$): δ 8.61 (s, 1H), 8.43 (d, 1H, J = 7.6 Hz), 7.96 (d, 1H, J = 8 Hz), 4.56 (bt, 2H, J = 4.2 Hz), 3.84 (bt, 2H, J = 4.2 Hz), 3.68 (cm, 6H), 3.60 (b, 2H). ^{13}C NMR (100 MHz, $CDCl_3$): δ 162.9, 145.3, 142.7, 135.0, 134.9, 126.6, 125.5, 72.6, 70.8, 70.4, 68.9, 65.6, 61.8 ppm. HRMS (ESI, m/z): calcd for $C_{13}H_{16}N_2O_9Na$ $(M + Na)^+$ 367.0753; found 367.0756.

2-Mercaptoethyl 4-Chloro-3-nitrobenzoate (8-Cl). This was prepared by general procedure G from CNBA (1 g, 4.96 mmol) in 10 mL of β-mercaptoethanol. Elution over silica (ethyl acetate/hexanes 20%) afforded the thiol as an off-white solid in 25% yield (324 mg). MW: 261.68 g/mol. TLC: 50% ethyl acetate/hexanes, R_f = 0.50. ^{1}H NMR (400 MHz, $CDCl_3$): δ 8.46 (d, 1H, J = 2 Hz), 8.14 (dd, 1H, J_1 = 8.4 Hz, J_2 = 2 Hz), 7.62 (d, 1H, J = 8.4 Hz), 4.45 (t, 2H, J = 6.7 Hz), 2.87 (dt, 2H, J_1 = 8.6 Hz, J_2 = 6.7 Hz), 1.52 (t, 1H, J = 8.6). ^{13}C NMR (100 MHz, $CDCl_3$): δ 163.5, 148.0, 133.8, 132.4, 132.0, 129.9, 126.7, 67.2, 23.3 ppm. HRMS (ESI, m/z): calcd for $C_9H_9ClNO_4S$ $(M + H)^+$ 261.9941; found 261.9923. Mp: 60−62 °C.

2-Mercaptoethyl 3,4-Dinitrobenzoate (8-NO$_2$). This was prepared by general procedure G from DNBA (506 mg, 2.39 mmol) in 10 mL of β-mercaptoethanol. Elution over silica (ethyl acetate/hexanes 20%) afforded the thiol as an orange oil in 6% yield (39 mg). MW: 272.23 g/mol. ^{1}H NMR (400 MHz, $CDCl_3$): δ 8.56 (d, 1H, J = 1.6 Hz), 8.41 (dd, 1H, J_1 = 8.4 Hz, J_2 = 1.6 Hz), 7.97 (d, 1H, J = 8.4 Hz), 4.51 (t, 2H, J = 6.7 Hz), 2.91 (dt, 2H, J_1 = 8.6 Hz, J_2 = 6.7 Hz), 1.53 (t, 1H, J = 8.6). ^{13}C NMR (100 MHz, $CDCl_3$): δ 162.5, 145.5, 142.7, 134.9, 134.8, 126.5, 125.6, 67.8, 23.2 ppm. HRMS (ESI, m/z): $C_9H_8N_2O_6S$ calcd for $(M)^+$ 272.0103; found 272.0105.

2-(Prop-2-yn-1-yloxy)ethanol (9). Ether **9** was prepared from ethylene glycol and propargyl bromide in one step by a previously published method[34] (146 mg, 35% yield). The identity of **9** was confirmed by ^{1}H and ^{13}C NMR. Purity of **9** was determined by ^{1}H NMR and TLC. Physical and spectroscopic data were found to match literature data.[34]

2-(2-(2-(Prop-2-yn-1-yloxy)ethoxy)ethoxy)ethanol (10). Ether **10** was prepared from triethylene glycol and propargyl bromide in one step by a previously published method[45] (133 mg, 17% overall yield). The identity of **10** was confirmed by ^{1}H and ^{13}C NMR. The purity of **10** was determined by ^{1}H NMR and TLC. Physical and spectroscopic data were found to match literature data.[45]

Prop-2-yn-1-yl 4-Chloro-3-nitrobenzoate (11-Cl). This was prepared by general procedure H from CNBA (1 g, 4.96 mmol) in 10 mL of propargyl alcohol. The ester was obtained as an off-white powder in 96% yield (1.14 g) by elution over silica gel (20% ethyl acetate/hexanes) and recrystallization from boiling ethyl acetate. MW: 239.61 g/mol. TLC: 20% ethyl acetate/hexanes, R_f = 0.33. ^{1}H NMR (400 MHz, $CDCl_3$): δ 8.55 (d, 1H, J = 2.2 Hz), 8.18 (dd, 1H, J_1 = 8.4 Hz, J_2 = 2.2 Hz), 7.65 (d, 1H, J = 8.4 Hz), 4.95 (d, 2H, J = 2.8), 2.55 (t, 1H, J = 2.8 Hz). ^{13}C NMR (100 MHz, $CDCl_3$): δ 163.2, 148.1, 133.9, 132.5, 132.3, 129.5, 126.9, 76.1, 53.6 ppm. HRMS (ESI, m/z): calcd for $C_{10}H_7ClNO_4$ (M + H − acetylene radical)$^+$ 216.0064; found 216.0056. Mp: 68−70 °C.

Prop-2-yn-1-yl 3,4-Dinitrobenzoate (11-NO$_2$). This was prepared by general procedure H from DNBA (250 mg, 1.18 mmol) in 5 mL of propargyl alcohol. Elution of the residue over silica gel (20% ethyl acetate/hexanes) afforded the ester as a crystalline yellow solid in 41% yield (121 mg). MW: 250.16 g/mol. TLC: 50% ethyl acetate/hexanes, R_f = 0.53. ^{1}H NMR (400 MHz, $CDCl_3$): δ 8.60 (d, 1H, J = 1.6 Hz), 8.43 (dd, 1H, J_1 = 8.4 Hz, J_2 = 2 Hz), 7.97 (d, 1H, J = 8.4 Hz), 4.99 (d, 2H, J = 2.4 Hz), 2.58 (t, 1H, J = 2.4 Hz). ^{13}C NMR (100 MHz, $CDCl_3$): δ 162.1, 145.5, 142.7, 135.0, 134.4, 126.7, 125.6, 76.5, 54.2 ppm. HRMS (ESI, m/z): calcd for $C_{10}H_6N_2O_6$ (M^+) 250.0226; found 250.0212. Mp: 79−80 °C.

2-(Prop-2-yn-1-yloxy)ethyl 4-Chloro-3-nitrobenzoate (12-Cl). This was prepared by general procedure I from 2-(prop-2-yn-1-yloxy)ethanol (ether **9**, 229 mg, 2.3 mmol) and CNBA (614 mg, 1.3 equiv). The residue was purified by column chromatography (20% ethyl acetate/hexanes) to afford the ester as a yellow oil in 35% yield (228 mg). MW: 283.66 g/mol. TLC: 50% ethyl acetate/hexanes, R_f = 0.45. ^{1}H NMR (400 MHz, $CDCl_3$): δ 8.48 (d, 1H, J = 2 Hz), 8.14 (dd, 1H, J_1 = 8.4 Hz, J_2 = 2 Hz), 7.61 (d, 1H, J = 8.4 Hz), 4.50 (t, 2H, J = 4.6 Hz), 4.19 (d, 2H, J = 2.4 Hz), 3.85 (t, 2H, J = 4.6 Hz), 2.44 (t, 1H, J = 2.4). ^{13}C NMR (100 MHz, $CDCl_3$): δ 163.8, 148.0, 133.9, 132.3, 131.8, 130.1, 126.8, 79.3, 75.3, 67.4, 65.0, 58.5 ppm. HRMS (ESI, m/z): calcd for $C_{12}H_{11}ClNO_5$ $(M + H)^+$ 284.0326; found 284.0326.

2-(Prop-2-yn-1-yloxy)ethyl 3,4-Dinitrobenzoate (12-NO$_2$). This was prepared by general procedure I from 2-(prop-2-yn-1-yloxy)ethanol (ether **9**, 184 mg, 1.84 mmol) and DNBA (503 mg, 1.3 equiv). The residue was eluted over silica gel (ethyl acetate/hexanes 20%) to give the ester as an orange-brown oil in 79% yield (428 mg). MW: 294.22 g/mol. TLC: 50% ethyl acetate/hexanes, R_f = 0.33. ^{1}H NMR (400 MHz, $CDCl_3$): δ 8.58 (d, 1H, J = 1.6 Hz), 8.42 (dd, 1H, J_1 = 8.4 Hz, J_2 = 1.6 Hz), 7.96 (d, 1H, J = 8.4 Hz), 4.56 (m, 2H), 4.21 (d, 2H, J = 2.4 Hz), 3.88 (m, 2H), 2.46 (t, 1H, J = 2.4 Hz). ^{13}C NMR (100 MHz, $CDCl_3$): δ 162.7, 145.2, 142.5, 135.0, 134.8, 126.4, 125.5,

dx.doi.org/10.1021/jo401278x | J. Org. Chem. 2013, 78, 9647−9658

79.2, 75.2, 67.2, 65.5, 58.4 ppm. HRMS (ESI, m/z): calcd for $C_{12}H_{11}N_2O_7$ $(M + H)^+$ 295.0566; found 295.0553.

2-(2-(2-(Prop-2-yn-1-yloxy)ethoxy)ethoxy)ethyl 4-Chloro-3-nitrobenzoate (13-Cl). This was prepared by general procedure I from 2-(2-(2-(prop-2-yn-1-yloxy)ethoxy)ethoxy)ethanol (ether **10**, 249 mg, 1.3 mmol) and CNBA (348 mg, 1.3 equiv). The residue was eluted over silica gel (50% ethyl acetate/hexanes) to afford the ester as yellow oil in 72% yield (348 mg). MW: 371.77 g/mol. TLC: 50% ethyl acetate/hexanes, R_f = 0.29. ^{1}H NMR (400 MHz, $CDCl_3$): δ 8.40 (d, 1H, J = 2 Hz), 8.09 (dd, 1H, J_1 = 8.4 Hz, J_2 = 2 Hz), 7.57 (d, 1H, J = 8.4 Hz), 4.42 (t, 2H, J = 4.8 Hz), 4.08 (d, 2H, J = 2.4 Hz), 3.76 (t, 2H, J = 4.8 Hz), 3.58 (cm, 8H), 2.37 (t, 1H, J = 2.4 Hz). ^{13}C NMR (150 MHz, $CDCl_3$): δ 163.6, 147.8, 133.7, 132.2, 131.5, 130.1, 126.6, 79.6, 74.7, 70.6, 70.6, 70.4, 69.0, 68.9, 65.1, 58.3 ppm. HRMS (ESI, m/z): calcd for $C_{16}H_{18}ClNO_7Na$ $(M + Na)^+$ 394.0670; found 394.0681.

2-(2-(2-(Prop-2-yn-1-yloxy)ethoxy)ethoxy)ethyl 3,4-Dinitrobenzoate (13-NO_2). This was prepared by general procedure I from 2-(2-(2-(prop-2-yn-1-yloxy)ethoxy)ethoxy)ethanol (ether **10**, 200 mg, 1.1 mmol) and DNBA (292 mg, 1.3 equiv). The residue was eluted over silica gel (60% ethyl acetate/hexanes) to afford the ester as an orange-brown oil in 80% yield (336 mg). MW: 382.32 g/mol. TLC: 50% ethyl acetate/hexanes, R_f = 0.15. ^{1}H NMR (400 MHz, $CDCl_3$): δ 8.59 (d, 1H, J = 2 Hz), 8.42 (dd, J_1 = 8 Hz, J_2 = 2 Hz), 7.97 (d, 1H, J = 8 Hz), 4.55 (t, 2H, J = 4.8 Hz), 4.17 (d, 2H, J = 2.4 Hz), 3.84 (t, 2H, J = 4.8 Hz), 3.67 (cm, 8H), 2.40 (t, 1H, J = 2.4 Hz). ^{13}C NMR (100 MHz, $CDCl_3$): δ 162.5, 144.9, 142.2, 134.9, 134.7, 126.2, 125.4, 79.5, 74.6, 70.4, 70.4, 70.2, 68.9, 68.5, 65.5, 58.1 ppm. HRMS (ESI, m/z): calcd for $C_{16}H_{18}N_2O_9Na$ $(M + Na)^+$ 405.0910; found 405.0912.

Imidazole-1-sulfonyl Azide, Hydrochloride Salt. This was prepared from sulfuryl chloride, imidazole, and sodium azide by a previously published method[46] (23.9 g, 57% yield). The identity of **26** was confirmed by ^{1}H and ^{13}C NMR. The purity of this salt was determined by ^{1}H NMR and TLC. Physical and spectroscopic data were found to match literature data.[46]

6-Azidohexanoic Acid (6-AHA). Following a procedure from Goddard-Borger and Stick,[46] diazotransfer reagent salt (from above) (2.5 g, 1.2 equiv) was added to a stirred slurry of 6-aminohexanoic acid (1.3 g, 10 mmol), potassium carbonate (3 g, 2.2 equiv), and copper sulfate pentahydrate (67 mg, 2.7 mol %) in 50 mL of methanol and stirred at room temperature overnight. The methanol was then removed in vacuo, and 100 mL of water was added and carefully acidified by the addition of concentrated HCl (2 mL). The solution was then extracted with ether (5 × 20 mL), and the combined organic layers were dried with $MgSO_4$, filtered, and evaporated under reduced pressure to give the product as a pale yellow oil in 95% yield (1.49 g). MW: 157.17 g/mol. TLC: 50% ethyl acetate/hexanes, R_f = 0.46. ^{1}H NMR (400 MHz, $CDCl_3$): δ 11.2 (bs, 1H), 3.26 (t, 2H, J = 6.8 Hz), 2.36 (t, 2H, J = 7.4 Hz), 1.69−1.57 (cm, 4H), 1.45−1.37 (m, 2H). ^{13}C NMR (100 MHz, $CDCl_3$): δ 179.9, 51.3, 34.0, 28.7, 26.3, 24.3 ppm. FTIR thin film ν_{max}: 3277 (broad), 2943, 2871, 2098, 1711, 1373, 1284, 1256, 1187 cm^{-1}.

Enzymology and Detection of Products. The conjugation reactions of each substrate to GSH were studied as described previously.[25] The enzymatic and nonenzymatic conjugations of GSH to each substrate were observed.

a. Conjugations with SjGST. A typical reaction contained 2.85 mL of 20 mM sodium phosphate buffer (pH 7.0), 5 mM reduced glutathione, and 0.3 μM GST from *Schistosoma japonicum* ("enzymatic reaction solution"). The reaction was initiated by adding 150 μL of a 10 mM solution of the electrophile in methanol to the premixed buffer solution containing GSH and *Sj*GST. The mixture was incubated with stirring at 25 °C overnight, and then the UV−vis absorption spectrum was taken at 25 °C. For the reaction mixtures of enzymatic reactions, the absorbance was intense that a 1:100 dilution of the reaction solution with phosphate buffer was required to obtain measurements to conform to Beer's law (with OD well below 1.0).

b. Without SjGST. Nonenzymatic reactions were studied using the same protocol as above, but without the addition of *Sj*GST.

Reverse-Phase Liquid Chromatography−Mass Spectrometry. Enzymatic reactions were performed as described, and the crude reaction mixtures were subjected to reverse-phase LC−MS on a C-18 column. Thirty microliters of the conjugate solution was eluted on a gradient (1%−50% methanol/water with 0.05% formic acid over 15 min), and then with isocratic flow for 45 more minutes. Masses were observed via electrospray ionization (positive ion mode).

Determination of Extinction Coefficients for GSH−Electrophile Conjugates. The enzymatic reaction solution from the conjugation assay described above was used. Methanolic solutions of the electrophile to be studied were prepared by serial dilution and added to the enzyme-containing buffer to give final concentrations of electrophile ranging from 0.0625 to 1.25 mM (or lower, depending on the aqueous solubility of the substrate.) Vials were also prepared without enzyme to serve as controls. All reactions were incubated at 37 °C overnight, and the UV−vis absorbance measured for each solution at 356 nm. The difference in absorbance between the enzymatic and nonenzymatic reactions at each substrate concentration was plotted against substrate concentration to give a standard curve whose slope equals the extinction coefficient of the GSH−electrophile conjugate.

Determination of Michaelis−Menten Parameters for Electrophiles (Table 1). The enzymatic reaction solution was prepared as described above. To 2.85 mL of this solution was added 0.15 mL of a methanol solution of the electrophile to be studied to give final concentrations of electrophile in solution ranging from 4 to 0.31 mM. The initial rates were measured by observing the change in absorbance at 356 nm every minute for 10 min, then calculating the average change in optical density per minute. These measurements were taken in triplicate and averaged. Plotting the inverse of the obtained initial rates versus substrate concentration produced a Lineweaver−Burk plot from which were obtained the Michaelis−Menten parameters K_m and V_{max}. A direct fit of the data using plotting software was not possible because the substrates were significantly insoluble in the reaction buffer at concentrations approaching K_m.

Preparation of Electrophile-Modified Slides. After each step, the hydrophobicity of the surface was observed via contact-angle microscopy.

a. Modification with Azide Linker. Ordinary glass microscope slides were first cleaned by incubation in hot piranha solution (3:1 H_2SO_4:H_2O_2) for 30 min, rinsed with ethanol and deionized water, and dried overnight in a 200 °C oven. The slides were next silanized by incubation with a 10% (v/v) solution of 3-aminopropyltriethoxysilane (APTES) in ethanol at room temperature for 2 h, with shaking. The slides were then sonicated in ethanol for 10 min, rinsed with ethanol and deionized water, and then dried in a 200 °C oven for 2 h. The aminated slides were next incubated in a 1:1 solution of 10 mM each diisopropylcarbodiimide (DIC) and 6-azidohexanoic acid (synthesis described above) in methylene chloride for 18 h at room temperature with shaking. The slides were cleaned by sonicating in ethanol for 15 min, and then rinsing with ethanol, deionized water, and ethanol again.

b. "Click" Immobilization of Electrophiles. A "click" reaction solution consisting of 1 mM alkyne **13-Cl**, 100 mg of $CuSO_4 \cdot 5H_2O$, and 175 mg of sodium ascorbate in 50 mL of 1:1 H_2O:DMSO was applied to azide-modified slides, and the slides were incubated at room temperature with shaking for 4 h. The slides were rinsed with deionized water and sonicated for 10 min. These slides were subsequently used for the immobilization steps.

GSH-Conjugation and *Sj*GST Immobilization. A silicone isolator pad was pressed onto the CDNB-analogue modified slides to create 24 wells per slide. The enzymatic reaction solution described above was applied to the wells, and the slides were incubated at room temperature overnight, then rinsed several times with 20 mM phosphate buffer (pH 7.0) and allowed to air-dry.

Immunoassay-Based Detection of Immobilized *Sj*GST Protein. *a. Primary Antibody Labeling.* GST-tagged slides were first blocked with 5% bovine serum albumin (BSA) in 1x phosphate-buffered saline (PBS) containing 0.05% Tween 20 detergent (pH 7.3) for 30 min. Several dilutions of a mouse anti-GST primary antibody were prepared in blocking solution (1:10, 1:100, 1:1000, and 1:10 000 dilutions), and 3.5 μL of antibody solution was applied to each well on

dx.doi.org/10.1021/jo401278x | J. Org. Chem. 2013, 78, 9647−9658

the slide, which was incubated for 1 h at room temperature. The slides were then washed four times with PBS-Tween 20.

b. Secondary Antibody Labeling. 5 μL per well of a 1:200 dilution of goat antimouse IgG labeled with Texas Red in blocking solution was applied to the slide, which was incubated for 1 h at room temperature. The silicone isolator pad was removed, and the slides were washed four times with 1x PBS-Tween 20 (0.05%, pH 7.3) and air-dried.

■ ASSOCIATED CONTENT

Supporting Information

General experimental details, copies of ^{1}H and ^{13}C NMR spectra for all new compounds, UV−vis spectra for enzyme-catalyzed reactions, HPLC (LC−MS) chromatograms, and UV−vis and mass spectra of conjugates. This material is available free of charge via the Internet at http://pubs.acs.org.

■ AUTHOR INFORMATION

Corresponding Author

*E-mail: rajesh.viswanathan@case.edu.

Notes

The authors declare no competing financial interest.

■ ACKNOWLEDGMENTS

This work is dedicated to John A. Widtsoe Distinguished Professor C. Dale Poulter, University of Utah, on the occasion of his 70th birthday. We thank Case Western Reserve University for funding this study. We thank Dr. Dale Ray (CWRU) for assistance with NMR. We thank Dr. Jon Karty (Indiana University) for assistance with mass spectrometry. We thank Prof. Gregory Tochtrop (CWRU, Chemistry) for providing access to Shimadzu LC−MS analyzer. We thank Prof. C. Dale Poulter (University of Utah) and Dr. Jin Soo Seo (University of Utah) for generously gifting metallic chamber used for glass surface modifications. We thank Prof. John Mieyal (CWRU, Pharmacology) for generously gifting anti-GST antibody and for providing clarification on kinetic constants measured in this work.

■ REFERENCES

(1) Zhu, H.; Bilgin, M.; Bangham, R.; Hall, D.; Casamayor, A.; Bertone, P.; Lan, N.; Jansen, R.; Bidlingmaier, S.; Houfek, T.; Mitchell, T.; Miller, P.; Dean, R. A.; Gerstein, M.; Snyder, M. *Science* **2001**, *293*, 2101−2105.

(2) Mrksich, M.; Whitesides, G. M. *Annu. Rev. Biophys. Biomol. Struct.* **1996**, *25*, 55−78.

(3) MacBeath, G.; Schreiber, S. L. *Science* **2000**, *289*, 1760−1763.

(4) MacBeath, G. *Nat. Genet.* **2002**, *32*, 526−532.

(5) Kawahashi, Y.; Doi, N.; Takashima, H.; Tsuda, C.; Oishi, Y.; Oyama, R.; Yonezawa, M.; Miyamoto-Sato, E.; Yanagawa, H. *Proteomics* **2003**, *3*, 1236−1243.

(6) Gurard-Levin, Z. A.; Mrksich, M. *Annu. Rev. Anal. Chem.* **2008**, *1*, 767−800.

(7) Choudhuri, S. *J. Biochem. Mol. Toxicol.* **2004**, *18*, 171−179.

(8) Foong, Y. M.; Fu, J. Q.; Yao, S. Q.; Uttamchandani, M. *Curr. Opin. Chem. Biol.* **2012**, *16*, 234−242.

(9) Gerlt, J. A.; Allen, K. N.; Almo, S. C.; Armstrong, R. N.; Babbitt, P. C.; Cronan, J. E.; Dunaway-Mariano, D.; Imker, H. J.; Jacobson, M. P.; Minor, W.; Poulter, C. D.; Raushel, F. M.; Sali, A.; Shoichet, B. K.; Sweedler, J. V. *Biochemistry* **2011**, *50*, 9950−9962.

(10) Marin, V. L.; Bayburt, T. H.; Sligar, S. G.; Mrksich, M. *Angew. Chem., Int. Ed.* **2007**, *46*, 8796−8798.

(11) Schena, M.; Shalon, D.; Davis, R. W.; Brown, P. O. *Science* **1995**, *270*, 467−470.

(12) Walsh, C. T. *Posttranslational Modification of Proteins: Expanding Nature's Inventory*; Roberts and Co. Publishers: Greenwood Village, CO, 2006.

(13) Jonkheijm, P.; Weinrich, D.; Schroder, H.; Niemeyer, C. M.; Waldmann, H. *Angew. Chem., Int. Ed.* **2008**, *47*, 9618−9647.

(14) Gauchet, C.; Labadie, G. R.; Poulter, C. D. *J. Am. Chem. Soc.* **2006**, *128*, 9274−9275.

(15) Rashidian, M.; Song, J. M.; Pricer, R. E.; Distefano, M. D. *J. Am. Chem. Soc.* **2012**, *134*, 8455−8467.

(16) Agarwal, P.; van der Weijden, J.; Sletten, E. M.; Rabuka, D.; Bertozzi, C. R. *Proc. Natl. Acad. Sci. U.S.A.* **2013**, *110*, 46−51.

(17) Stephanopoulos, N.; Francis, M. B. *Nat. Chem. Biol.* **2011**, *7*, 876−884.

(18) Borra, R.; Dong, D.; Elnagar, A. Y.; Woldemariam, G. A.; Camarero, J. A. *J. Am. Chem. Soc.* **2012**, *134*, 6344−6353.

(19) Johnsson, N.; Johnsson, K. *ChemBioChem* **2003**, *4*, 803−810.

(20) Smith, D. B.; Johnson, K. S. *Gene* **1988**, *67*, 31−40.

(21) Giepmans, B. N. G.; Adams, S. R.; Ellisman, M. H.; Tsien, R. Y. *Science* **2006**, *312*, 217−224.

(22) Kolodziej, C. M.; Chang, C. W.; Maynard, H. D. *J. Mater. Chem.* **2011**, *21*, 1457−1461.

(23) Chang, C. W.; Nguyen, T. H.; Maynard, H. D. *Macromol. Rapid Commun.* **2010**, *31*, 1691−1695.

(24) Viswanathan, R.; Labadie, G. R.; Poulter, C. D. *Bioconjugate Chem.* **2013**, *24*, 571−577.

(25) Voelker, A. E.; Viswanathan, R. *Bioconjugate Chem.* **2013**, DOI: 10.1021/bc400128g.

(26) Sletten, E. M.; Bertozzi, C. R. *Angew. Chem., Int. Ed.* **2009**, *48*, 6974−6998.

(27) Armstrong, R. N. *Chem. Res. Toxicol.* **1997**, *10*, 2−18.

(28) Ji, X.; Armstrong, R. N.; Gilliland, G. L. *Biochemistry* **1993**, *32*, 12949−12954.

(29) Mannervik, B. *J. Biol. Chem.* **2012**, *287*, 6072−6083.

(30) Habig, W. H.; Pabst, M. J.; Jakoby, W. B. *J. Biol. Chem.* **1974**, *249*, 7130−7139.

(31) Cardoso, R. M. F.; Daniels, D. S.; Bruns, C. M.; Tainer, J. A. *Proteins* **2003**, *51*, 137−146.

(32) Atkinson, H. J.; Babbitt, P. C. *Biochemistry* **2009**, *48*, 11108−11116.

(33) Dess, D. B.; Martin, J. C. *J. Org. Chem.* **1983**, *48*, 4155−4156.

(34) Harada, T.; Muramatsu, K.; Mizunashi, K.; Kitano, C.; Imaoka, D.; Fujiwara, T.; Kataoka, H. *J. Org. Chem.* **2008**, *73*, 249−258.

(35) Lo, W. J.; Chiou, Y. C.; Hsu, Y. T.; Lam, W. S.; Chang, M. Y.; Jao, S. C.; Li, W. S. *Bioconjugate Chem.* **2007**, *18*, 109−120.

(36) Keen, J. H.; Habig, W. H.; Jakoby, W. B. *J. Biol. Chem.* **1976**, *251*, 6183−6188.

(37) Busenlehner, L. S.; Alander, J.; Jegerscohld, C.; Holm, P. J.; Bhakat, P.; Hebert, H.; Morgenstern, R.; Armstrong, R. N. *Biochemistry* **2007**, *46*, 2812−2822.

(38) Hoog, J. O.; Holmgren, A.; D'Silva, C.; Douglas, K. T.; Seddon, A. P. *FEBS Lett.* **1982**, *138*, 59−61.

(39) Burg, D.; Mulder, G. J. *Drug Metab. Rev.* **2002**, *34*, 821−863.

(40) Fujikawa, Y.; Urano, Y.; Komatsu, T.; Hanaoka, K.; Kojima, H.; Terai, T.; Inoue, H.; Nagano, T. *J. Am. Chem. Soc.* **2008**, *130*, 14533−14543.

(41) Martos-Maldonado, M. C.; Casas-Solvas, J. M.; Tellez-Sanz, R.; Mesa-Valle, C.; Quesada-Soriano, I.; Garcia-Maroto, F.; Vargas-Berenguel, A.; Garcia-Fuentes, L. *Biochimie* **2012**, *94*, 541−550.

(42) Randl, S.; Blechert, S. *J. Org. Chem.* **2003**, *68*, 8879−8882.

(43) Bastian, J. A.; Lash, T. D. *Tetrahedron* **1998**, *54*, 6299−6310.

(44) Sen, S. E.; Roach, S. L. *Synthesis* **1995**, 756−758.

(45) Lu, G.; Lam, S.; Burgess, K. *Chem. Commun.* **2006**, *42*, 1652−1654.

(46) Goddard-Borger, E. D.; Stick, R. V. *Org. Lett.* **2007**, *9*, 3797−3800.